



Project Report

Investigating the Effectiveness of an IMU Portable Gait Analysis Device: An Application for Parkinson's Disease Management

Nikos Tsotsolas ^{1,2,*}, Eleni Koutsouraki ³, Aspasia Antonakaki ³, Stefanos Pizanias ¹, Marios Kounelis ¹, Dimitrios D. Piromalis ⁴, Dimitrios P. Kolovos ⁵, Christos Kokkotis ^{6,7,8}, Themistoklis Tsatalas ^{6,8}, George Bellis ⁶, Dimitrios Tsaopoulos ⁷, Paris Papaggelos ⁶, George Sidiropoulos ⁹ and Giannis Giakas ^{8,*}

¹ R&D Department, Pan Antistixis SA, 106 71 Athens, Greece; spizanias@pan-antistixis.com (S.P.); info@fullybooked.gr (M.K.)

² DigiT-DSS Lab, University of West Attica, 122 43 Egaleo, Greece

³ R&D Department, E. Koutsouraki & SIA E.E.—Knowledge Brokers, 152 38 Athens, Greece; ekoutsouraki@green-projects.gr (E.K.); san@knowledge-brokers.gr (A.A.)

⁴ Electrical and Electronics Engineering Department, University of West Attica, 122 43 Egaleo, Greece; piromali@uniwa.gr

⁵ INNOESYS P.C., 122 41 Egaleo, Greece

⁶ Biomechanical Solutions, 431 00 Karditsa, Greece; chkokkotis@gmail.com (C.K.); tsatalas@uth.gr (T.T.); ge.mpellis@gmail.com (G.B.); ppapangel@gmail.com (P.P.)

⁷ Center for Research and Technology Hellas, Institute for Bio-Economy and Agri-Technology, 382 21 Volos, Greece; d.tsaopoulos@certh.gr

⁸ Department of Physical Education & Sport Science, University of Thessaly, 421 00 Trikala, Greece

⁹ Department of Financial and Management Engineering, University of the Aegean, 821 00 Chios, Greece; gsidiropoulos@aegean.gr

* Correspondence: ntsotsolas@pan-antistixis.com (N.T.); ggiakas@gmail.com (G.G.)



Citation: Tsotsolas, N.; Koutsouraki, E.; Antonakaki, A.; Pizanias, S.; Kounelis, M.; Piromalis, D.D.; Kolovos, D.P.; Kokkotis, C.; Tsatalas, T.; Bellis, G.; et al. Investigating the Effectiveness of an IMU Portable Gait Analysis Device: An Application for Parkinson's Disease Management. *BioMedInformatics* **2024**, *4*, 1085–1096. <https://doi.org/10.3390/biomedinformatics4020061>

Academic Editors: Jose Salinas and Alexandre G. De Brevern

Received: 25 July 2023

Revised: 29 February 2024

Accepted: 20 March 2024

Published: 10 April 2024



Copyright: © 2024 by the authors. Licensee MDPI, Basel, Switzerland. This article is an open access article distributed under the terms and conditions of the Creative Commons Attribution (CC BY) license (<https://creativecommons.org/licenses/by/4.0/>).

Abstract: As part of two research projects, a small gait analysis device was developed for use inside and outside the home by patients themselves. The project PARMODE aims to record accurate gait measurements in patients with Parkinson's disease (PD) and proceed with an in-depth analysis of the gait characteristics, while the project CPWATCHER aims to assess the quality of hand movement in cerebral palsy patients. The device was mainly developed to serve the first project with additional offline processing, including machine learning algorithms that could potentially be used for the second aim. A key feature of the device is its small size (36 mm × 46 mm × 16 mm, weight: 14 g), which was designed to meet specific requirements in terms of device consumption restrictions due to the small size of the battery and the need for autonomous operation for more than ten hours. This research work describes, on the one hand, the new device with an emphasis on its functions, and on the other hand, its connection with a web platform for reading and processing data from the devices placed on patients' feet to record the gait characteristics of patients on a continuous basis.

Keywords: Parkinson's disease; wearable devices; data analysis platform; monitoring technologies; gait analysis

1. Introduction

The human upper and lower limbs, comprising the shoulders, arms, and hands at the top and thighs, calves, and feet at the bottom, respectively, are structures enabling a diverse array of movements essential for daily activities. The study of their movement provides a powerful tool through which researchers, clinicians, and engineers can investigate their function and importance. Parkinson's and cerebral palsy diseases have an immediate effect on the movement of these limbs; therefore, the significance of studying their biomechanics becomes particularly important. Individuals suffering from neurological disorders like Parkinson's and cerebral palsy experience medium to severe alterations in their foot and arm movement patterns. Biomechanical assessments enable clinicians to identify deficits,

asymmetries, and compensatory strategies, informing the development of tailored rehabilitation interventions. Whether rehabilitating from a stroke, recovering from a traumatic injury, or managing conditions like cerebral palsy, a thorough understanding of the biomechanics of upper and lower limb movement is indispensable for optimizing rehabilitation outcomes [1].

This study presents two projects. Firstly, the CPWATCHER project aims to quantify the quality of the arms movement of CP children. The second project, PARMODE, aims to quantify the movement of the lower limbs of Parkinsonian patients. Both projects needed a smart IMU sensor with different firmware. The developed hardware and software for the PARMODE project will be presented here.

Parkinson's disease (PD) is one of the most common neurodegenerative diseases and is accompanied by movement disorders often observed in neurological practice [2–5]. Khodakarami et al. [6] highlighted that this disease affects movement, cognition, and the nervous system, and causes neuropsychiatry. It is considered a complex multifactorial disease in which unknown environmental cues, genetic factors, and either causative or susceptible variants trigger the pathology [7]. The consequences are multi-dimensional. PD causes (1) direct and indirect costs for health services, (2) personalized care costs to adapt to changes in mobility conditions and in accommodation, (3) societal costs, given that productivity at work decreases, and (4) reduced quality of life and wellbeing issues [8]. In recent years, rapid technological advancements, such as the development of wearable sensors and smart mobile devices (smartphones and tablets) [9,10], allow clinicians to monitor and manage PD patients from a distance continuously and in real-time [11].

Previous studies have identified the research priorities for people with PD, including the improvement of motor and non-motor symptoms, interventions specific to Parkinson's disease, better monitoring systems, and quality health care [12,13]. People with Parkinson's disease have already expressed their desire for wearable devices to capture data on a range of symptoms and lifestyle factors. Ancona et al. [14] presented a systematic literature review which is focused on the different types of sensors and their placement on the body for measuring PD symptoms and concluded that there are still many research gaps for future work.

As part of the research project, a gait analyzer was developed to record accurate gait measurements, detect the freezing of gait (FOG) in real-time, and transmit visual and auditory stimuli (via Bluetooth technology) to lightweight smart glasses (e.g., google glasses) with a micro-screen to deal with the "kinesia paradoxa" phenomenon [15]. The device sends the measurement data as well as the results related to the characteristics of the gait analysis onto an electronic platform. Through the intensive use of visualization tools and a high level of data analysis both in real-time and retrospectively, the web platform enables the treating physician to monitor the patient's gait data.

A microcontroller-based device was developed, taking into consideration that such kind of devices have become very popular and their cost has dropped a lot [9]. Furthermore, their usage is increased when these devices are wirelessly connected to smart devices [10]. A key feature of the device that was developed is its small size, which creates specific requirements in terms of energy consumption restrictions due to the small size of the battery on one hand and the need for high autonomy on the other. For this reason, during the design of the firmware, procedures were provided for placing the sensors, the Bluetooth communication module, and the controller in a state of minimal (almost zero) consumption. In addition, special emphasis was placed on the design of the functions used to calculate the gait parameters to limit the resource consumption of the processor. Regarding the embedded software related to the gait analysis procedures, it supports the processing of the data from the devices that will be placed on the patient's feet to continuously record the data from the 3D accelerometer and 3D gyroscope and to process these data to calculate the gait characteristics of patients in real-time.

Specifically:

- Length of gait (m);

- Duration of gait (s);
- Speed of gait (m/s)

This information is sent through the mobile app to the web app for the calculation of additional gait analysis characteristics.

Specifically:

- Bilateral Parameters:
- Cadence (steps/min);
- Double Support (%)

Unilateral Parameters:

- Swing (%);
- Stance (%);
- Step Length (m)

The structure of this article is as follows: Section 2 describes the device hardware and embedded software in the processor to calculate the device’s basic parameters related to the gait analysis. Section 3 presents the mobile app that supports the operation of the devices and acts as a gateway for transferring the data to the web platform or other connected devices, such as smart glasses. In Section 4, the web platform is briefly presented, focusing on the section of gait analysis data per session. Section 5 refers to the evaluation of the information produced by the device compared to the corresponding information that is produced by the system LEGSys™ (Locomotion Evaluation and Gait System).

To summarize, the purpose of this study is to present a new wireless IMU system using one of the latest IMUs released in the market that will be used to study human movement.

2. Gait Analysis Device

The system consists of a pair of identical devices. One device is placed on the left leg and the other on the right leg of the patient.

The schematic of the board has a hierarchical structure. It is divided into subsystems to facilitate clarity and readability. At the top level of the schematic, as it is shown in Figure 1, subsystems are interconnected. We observe that the central subsystem of the microcontroller is located in the MCU_Display. SchDoc sheet is connected with the appropriate signals and with the rest of the sheets that contain the rest of the subsystems.

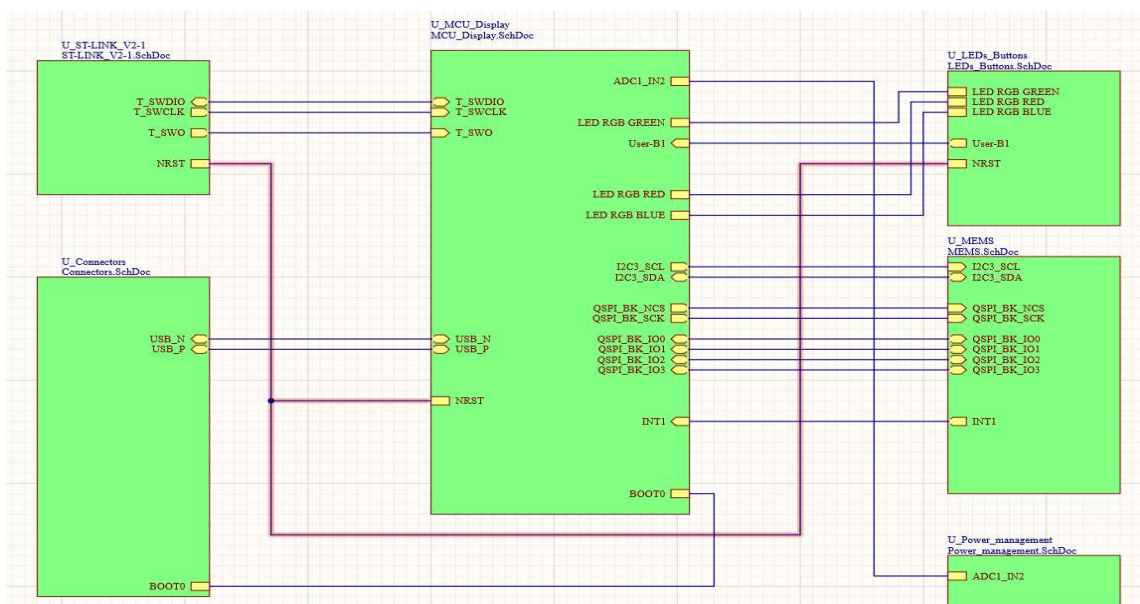


Figure 1. Flow processes diagram of the device’s firmware.

The individual subsystems are as follows:

1. Microcontroller/Bluetooth Low Energy;

This subsystem includes the microcontroller, which also performs the Bluetooth Low Energy (BLE) communication. STM32WB5MMGH6TR is a telecommunications module of the ST company that, apart from the microcontroller, also includes the necessary radio frequency circuits for the operation of the BLE as well as the antenna. As a microcontroller, STM32WB consists of two cores: one to execute the BLE protocol and one for the user application.

2. QSPI Flash Memory;

This subsystem includes the Flash memory in which the recording data are stored.

This is a 128 Mbit memory. Connected through the QSPI Interface at a frequency of up to 133 MHz, it has enough Bandwidth, so that the recording does not interfere with the sampling of the signals.

3. 3D accelerometer and 3D gyroscope;

ISM330DHCX is a high-performance 3D digital accelerometer and 3D digital gyroscope based on micro-mechanics, mounted on the same silicon matrix, ensuring superior stability and robustness.

It has a full-scale acceleration range of $\pm 2/\pm 4/\pm 8/\pm 16$ g and a wide angular rate range of $\pm 125/\pm 250/\pm 500/\pm 1000/\pm 2000/\pm 4000$ dps. Communication with the microcontroller is achieved through the I2C protocol.

4. Hardware User Interface;

The basic handling of the device is conducted through the mobile app. In addition, the device status is reflected on the integrated RGB LED. At the same time, a Reset button and one for the application use are provided to facilitate the use of the device.

5. USB Port;

USB port is primarily the power source of the device but is also available for any wired communication that may be needed.

6. Battery power and charging;

Texas Instruments integrated BQ24232 is a specialized monolithic Li-Ion battery charger. It takes power from the USB port and charges the single-cell battery. At the same time, it also performs "Power Path" functions, i.e., manages where the system will be powered, either from the USB or battery. A small linear voltage regulator ensures that the system voltage does not exceed 3.3 V.

7. Debug Port;

Debugging and programming of the hardware (firmware) are carried out through the Serial Wire Debug interface of the microcontroller.

The need for the device to be worn on the patient's legs led to a very "tight" design with small tolerances and components, resulting in a small and light product. For the same reason, both sides of the board were used to mount the components, thus saving the board area.

The final board dimensions are 27.4 mm \times 30.4 mm. For the board to be held in the SMD machines, two strips were added on the right and left, which were easily removed after manufacturing due to the pre-scoring (scoring) that they have on their borders.

Apart from the small tolerances, another feature that makes this board relatively difficult to manufacture is the "Filled Vias" manufacturing technique which is required to connect the internal pads of the BLE module.

Due to the presence of fast signals on the board, the "Via stitching" design technique was used to strongly join the copper levels of the earth in many places, which is also useful for shielding and isolating the board's signals.

Figure 2 shows the structure of the code sections that manage the peripherals and various basic functions of the system. Figure 3 shows the final version of the device.



Figure 2. Structure diagram of driver's software 1.0.



Figure 3. The final version of the device.

3. App

The App for mobile devices was developed specifically to support the devices' operation and acts as a gateway for transferring the data to the web platform or other connected devices. By entering the application, the user can connect the two devices, placed on the left and right foot, respectively, via Bluetooth. Firstly, in order to make the connection, the mobile phone's Bluetooth must be active and the two measurement devices must be active and charged (green light). The successful connection between these two devices is shown on the mobile screen (Figure 4).

After connecting by pressing each gear, the devices are calibrated (old data are deleted and the current date is set), which takes a few seconds. As soon as the measurement (calibration) is finished, the Ready to Start button appears (Figure 4).

The button starts the recording of measurements. The timer shows the duration of the recording session. As long as the recording lasts, the button on the top right (radar) is activated, and when it is pressed, the function of the current data starts (speed) (Figure 5).

After stopping the recording by pressing the "Read and Store" button at the bottom, data are sent to the web platform for further data analysis (Figure 5).

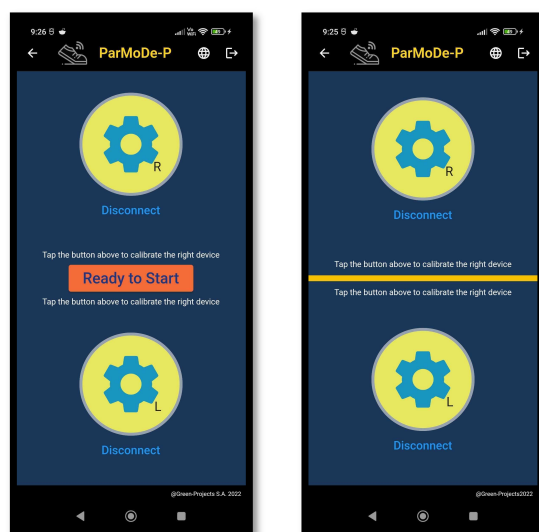


Figure 4. Successful connection between both devices.

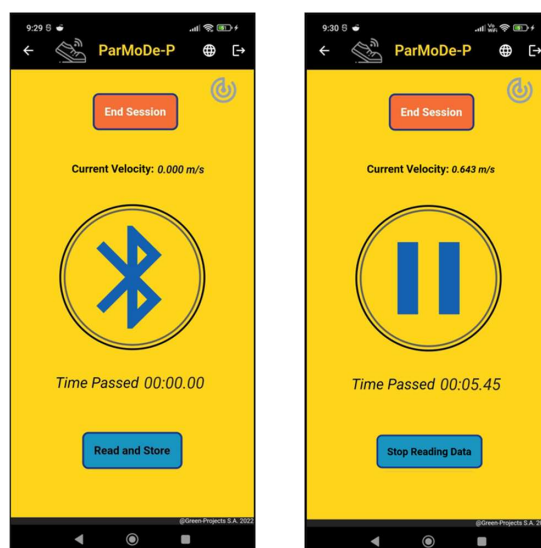


Figure 5. Read and send data.

4. Web Platform

In this section, the electronic platform that supports the remote monitoring and data analysis platform is presented (Remote Monitoring and Data Analysis Platform). The platform, through the use of visualization tools and data analysis tools both in real-time and retrospectively, enables the attending physician to monitor patients' gait data. The platform aims to facilitate the selection of the most effective treatment to be used for each patient. In addition, the platform allows the attending physician to monitor patients remotely, which helps to manage both the physician's and patients' time more efficiently.

The remote data monitoring and analysis platform performs and analyzes data sent via Bluetooth from the device to the back-end of the platform and provides interactive visualization of the patient's condition to offer a better interpretation of the patient's clinical picture. In addition, it can support further analysis of the progression of the disease, the intensity of the symptoms, the occurrence of ON-OFF periods, and the effectiveness of various treatments. On the platform, the collected data are divided into four sections:

1. Real-time (or almost real-time) data via a gait tracker;
2. Current state of Parkinsonian quality of life as recorded using standardized tools, such as the PDQ-39 and PDQ-83;

3. Current state of the patient’s clinical picture as recorded by the attending physician;
4. Recording of the treatments to which the patient is subjected in hospitals and special care centers.

The presentation section of the analysis of the patient’s walking data on the platform is of particular importance. More specifically, the connected devices and sessions in which the patient used the devices to record gait data are displayed per patient. The relevant screens present Velocity and Position charts in real-time as they are transferred from the devices through the mobile app (Figure 6). At this point, the user can save the desired data by exporting them to one of the six available forms.



Figure 6. Real-time data.

In the “Step Analysis” tab, the user can monitor the steps performed by the patient in the form of bar charts, where the orange boxes represent the Phase Stage of the patient’s movements, while the boxes with blue color represent the Swing Phase of the patient’s movements based on the selected time dimension during a walking cycle (Figure 7).

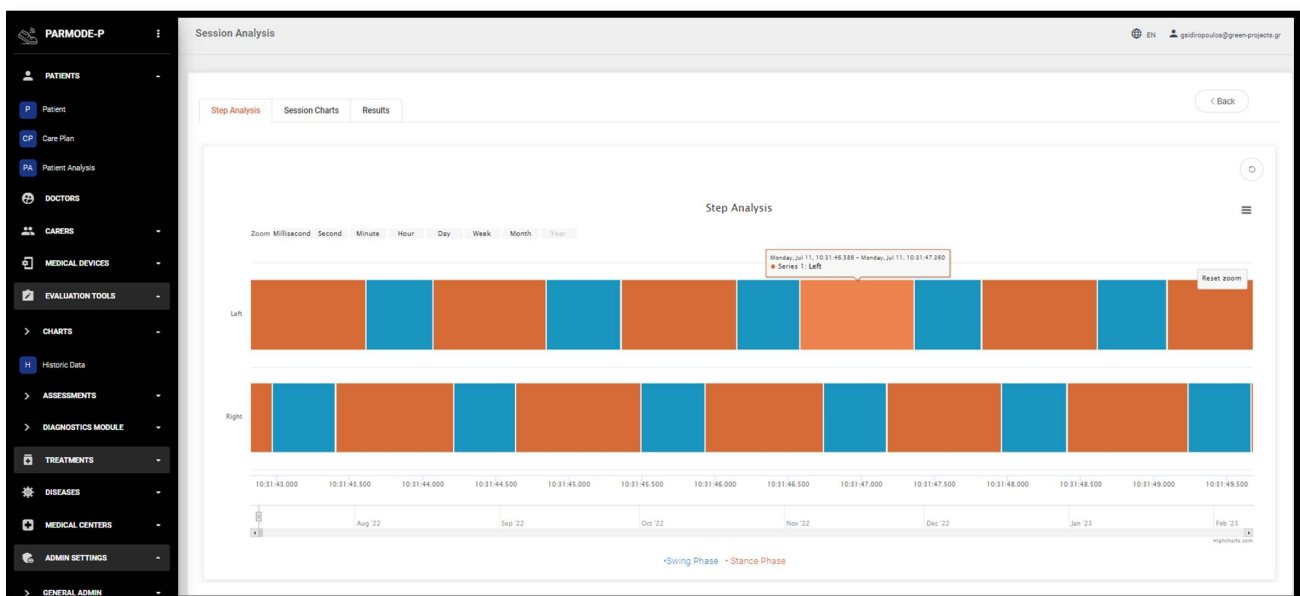


Figure 7. Step states.

In the “Session Charts” tab, the user can monitor the steps performed by the patient in the form of lines, where the orange-colored boxes represent the Velocity and Position of the patient’s movements (left and right device) based on the selected time dimension during a walking cycle (Figure 8).

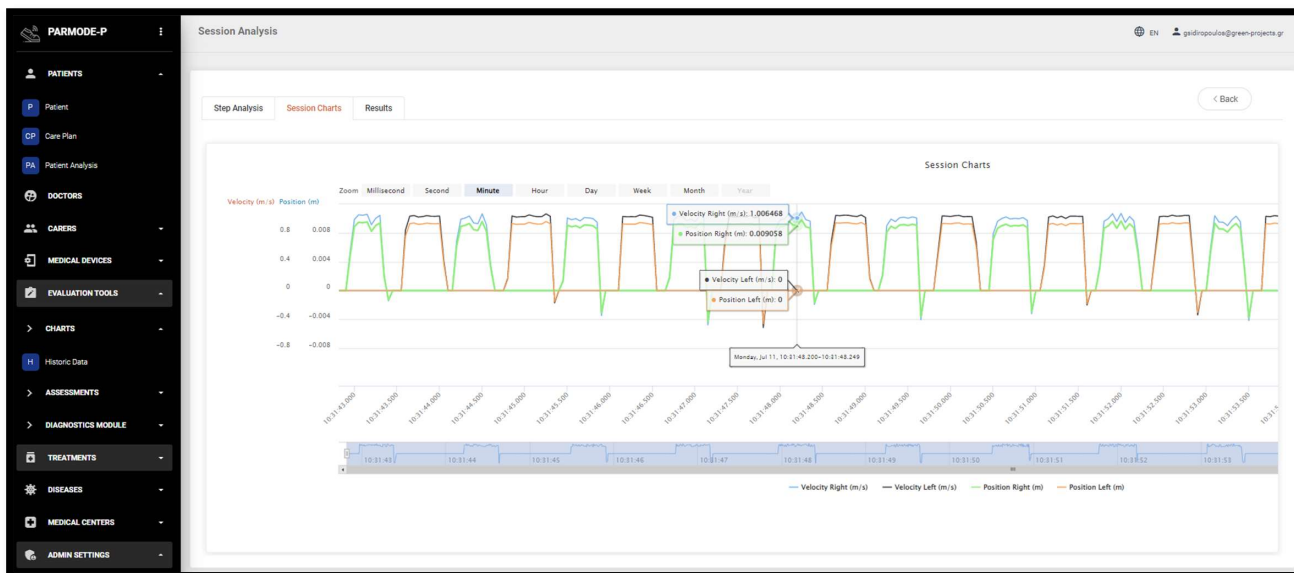


Figure 8. Data charts.

Finally, in the “Results” tab, the user can monitor the results in the form of tables, where the first table refers to the results of the Binary Parameters, and the second table refers to the results of the Monomeric Parameters during a walking cycle (Figure 9).

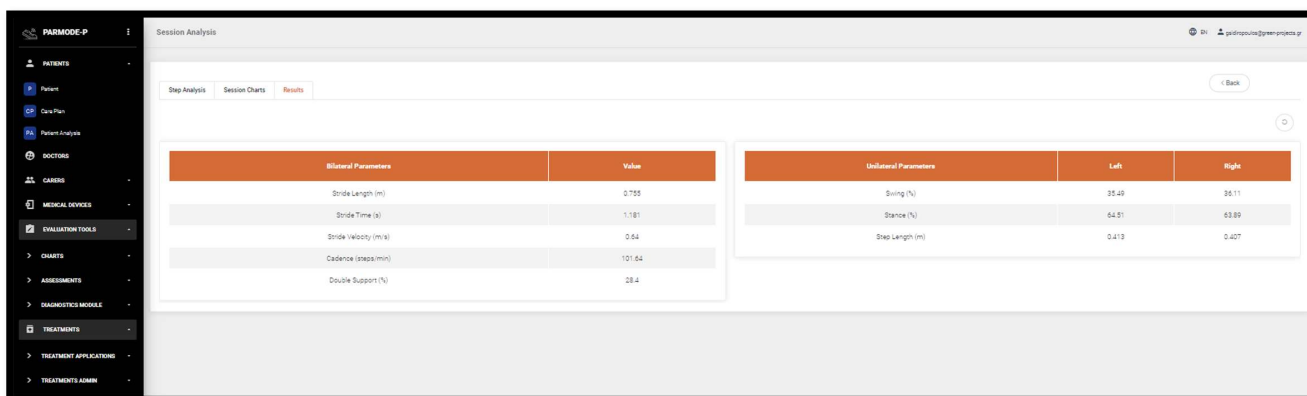


Figure 9. Gait analysis parameters.

5. Evaluation of Device Accuracy

We initially tested the random error and systematic error of the device when it was in complete silence status. The criterion of gravity was used (9.81 m/s^2) for the accelerometer values and 0 deg/s for the angular velocity values. The device was placed at several positions, and data were recorded at 100 Hz. The resultant 3D acceleration Acc_r was calculated (criterion 9.81 m/s^2) via the accelerometer component measurements ($Acc_x - Acc_y - Acc_z$) given from the device using the following formula:

$$Acc_r = \text{sqrt} (Acc_x^2 + Acc_y^2 + Acc_z^2)$$

Similarly, we calculated the absolute resultant angular velocity (criterion 0 deg/s).

When the system is in silence status, the level of accuracy in the acceleration is within 0.04 m/s^2 in the acceleration and within 0.01 deg/s in the angular velocity, which is evident (Figures 10 and 11) and within acceptable levels. Furthermore, if these data are to be compared with other devices that are available in the market, it will be shown that the ISM330DHCX sensor produces far more reliable and stable data, which could be examined in a future study.

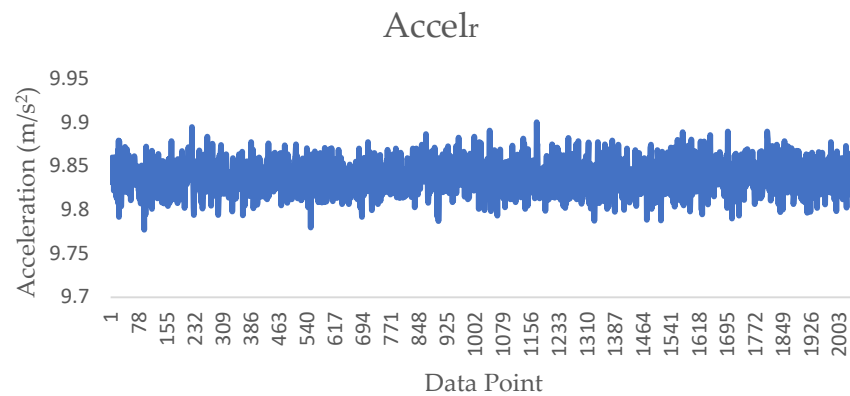


Figure 10. The resultant acceleration recorded and zoomed within the range of 9.70–9.95 to understand the level of accuracy of the system.

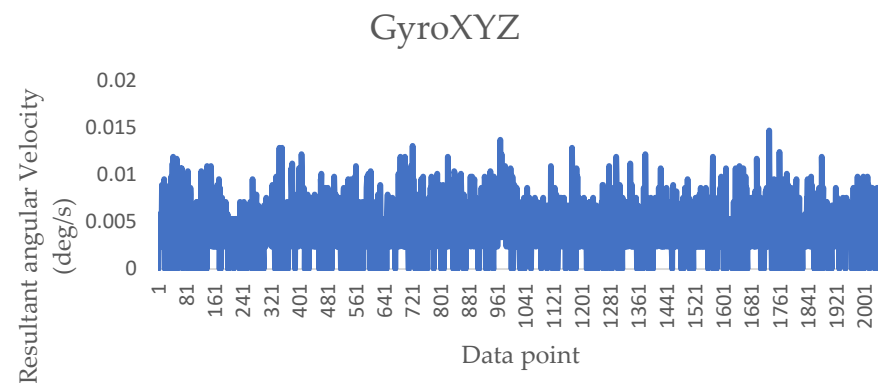


Figure 11. Absolute resultant angular velocity recorded and zoomed within the range of 0–0.02 to understand the level of accuracy of the system.

More reliable data are a distinctive factor in creating better algorithms for machine learning applications that are important for other studies, for example, the movement of the upper limbs in CP patients, as was the purpose of the CPWATCHER project that was briefly mentioned above.

In the context of the tests of the IMU device, a study was carried out on 25 patients, resulting in a total of 73 sets of measurements. The aim of this study was to correlate different indicators of the device in each patient separately with the corresponding measurements that were obtained simultaneously through the device LEGSys of BioSensics [16]. The following tests were selected:

- 10 m walk test (straight line);
- 10 m time up and go test;
- 10 m walk test (freeway)

The first two tests were repeated three times to ensure that the results obtained were accurate and reliable, and the respective averages were calculated.

The evaluation was mainly based on the comparison of the average values of indicators from the patients. Eight indicators were recorded for each patient based on the

measurements, and each measurement from the different systems led to the creation of two sets of samples per indicator.

Taking into account the international literature and decision charts for the selection of control statistical analysis, the Paired Samples parametric *t*-test [17] was selected to reject or accept the null hypothesis about whether the paired samples have a statistically significant relationship (*p*-value < 0.001), and subsequently, whether the difference of the means of the samples under comparison approaches zero. At this point, it should be noted that a normality test was carried out with the Kolmogorov–Smirnov test (N = 73), based on which the results were positive, allowing the *t*-test of these pairwise variables to be performed. Table 1 below provides a summary of Paired Samples parametric *t*-test results.

Table 1. *p*-values of Paired Samples parametric *t*-tests for each hypothesis between the comparison of PARMODE and control device data.

	Significance One-Sided <i>p</i>	Significance Two-Sided <i>p</i>
BP Stride Length (m)—BP Stride Length (m) (PL)	<0.001	<0.001
BP Stride Length (m)—BP Stride Length (m) (PL)	<0.001	<0.001
BP Stride Velocity (m/s)—BP Stride Velocity (m/s) (PL)	<0.001	<0.001
BP Cadence (steps/min)—BP Cadence (steps/min) (PL)	<0.001	<0.001
BP (Double Support (%)) and BP (Double Support (%)) (PL)	<0.001	<0.001
Swing (%) Left and Swing (%) Left (PL)	<0.001	<0.001
Stance (%) Left— Stance (%) Left (PL)	<0.001	<0.001
Step Length (m) Left— Step Length (m) Left (PL)	<0.001	<0.001
Swing (%) Right and Swing (%) Right (PL)	<0.001	<0.001
Stance (%) Right and Stance (%) Right (PL)	<0.001	<0.001
Stance (%) Right and Stance (%) Right (PL)	<0.001	<0.001

In addition, to verify the results, an analysis using the ANOVA method [18] was performed through the Compare Means command to reject or accept the null hypothesis regarding whether the paired samples have a statistically significant relationship (*p*-value > 0.001). Therefore, the difference of the means of the samples under comparison approaches zero. Table 2 below provides a summary of the ANOVA *p*-values results.

Table 2. Summary of ANOVA *p*-values for each hypothesis between the comparison of PARMODE and control device data.

	Sig.
BP Stride Length (m)	0.019
BP Stride Time (s)	0.0014
BP Stride Velocity (m/s)	0.002
BP Cadence (steps/min)	0.0012
BP (Double Support (%))	0.002
Swing (%) Left	0.003
Stance (%) Left	0.003
Step Length (m) Left	0.003
Swing (%) Right (PL) and Swing (%) Right	0.002
Stance (%) Right (PL) και Stance (%) Right	0.005
Step Length (m) Right	0.002

Finally, it is worth noting that for the 20th patient, an extreme value was observed in an index for which the statistical error was high. This value is due to the large deviation of the step in the right leg, mainly due to the possible difficulty of the patient to perform the step during the Stance Phase. For the gait analysis of each patient, eight motion analysis indices and their corresponding values were generated.

Limitations of this study include the small sample size of the measurements and the small number of patients who were involved in the processes of validation, with no

comparison to healthy controls. Potential limitations could be the comfort and ease of use for patients, which have not been investigated but also depend on the encapsulation of the device. A full-scale study is further needed to test the accuracy and validity of the device.

6. Conclusions

We developed an IMU device based on the ISM330DHCX chip from ST. This chip is a high-performance 3D digital accelerometer and 3D digital gyroscope based on micro-mechanics, mounted on the same silicon matrix, ensuring superior stability and robustness. Our initial tests show that its performance is superior to that of current devices available in the market, which are based on the previous generation of IMU sensors.

The conclusions of this research highlight important findings that emerged from the statistical analysis. More specifically, for the statistical analysis of the samples, since normality was checked, the appropriate methods were chosen (Paired Samples *t*-test and ANOVA). Considering the results obtained in the previous analyses, both the Paired Samples *t*-test and ANOVA test for each pair of variables that were examined from the device and control device (LEGSys) revealed statistically significant relationships between the samples for all parameters [19].

An important issue for further research relates to the exploitation of the collected data during the everyday use of the devices through the application of intelligent data analysis approaches using Machine Learning and Deep Learning techniques [20].

We did not run extensive comparisons with other devices. The basic tests that we ran showed excellent outcomes, but a more systematic study is needed in the future. It has to be mentioned that due to the latest unstable market conditions (chip crisis) coupled with the expansion of smart devices and smart cars, the ISM330DHCX sensor, along with other newly developed IMU sensors, was extinct for a long period, with the market now catching up.

Author Contributions: Conceptualization, N.T. and D.D.P.; methodology, D.D.P.; software, M.K. and S.P.; validation, G.B. and E.K.; formal analysis, C.K. and G.S.; resources, D.P.K.; writing—original draft preparation, D.T. and D.D.P.; writing—review and editing, T.T. and N.T.; visualization, P.P.; supervision, G.G. and N.T.; project administration, A.A.; funding acquisition, N.T., D.P.K., T.T. and E.K. All authors have read and agreed to the published version of the manuscript.

Funding: This research was co-financed by the European Regional Development Fund of the European Union and Greek national funds through the Operational Program Competitiveness, Entrepreneurship and Innovation, under the call RESEARCH-CREATE-INNOVATE (project codes: T1EDK-04022 and T2EDK-00759).

Institutional Review Board Statement: This study was conducted in accordance with the Declaration of Helsinki, and approved by the Institutional Ethics Committee of the University of Thessaly (protocol code 4-2 and 6-4-2022) for studies involving humans.

Informed Consent Statement: Informed consent was obtained from all subjects involved in the study.

Data Availability Statement: Data are available upon request.

Conflicts of Interest: The authors declare no conflicts of interest.

References

1. Slavens, B.A.; Harris, G.F. The biomechanics of upper extremity kinematic and kinetic modeling: Applications to rehabilitation engineering. *Crit. Rev. Biomed. Eng.* **2008**, *36*, 93–125. [[CrossRef](#)] [[PubMed](#)]
2. Poewe, W.; Seppi, K.; Tanner, C.M.; Halliday, G.M.; Brundin, P.; Volkman, J.; Schrag, A.E.; Lang, A.E. Parkinson disease. *Nat. Rev. Dis. Primers* **2017**, *3*, 17013. [[CrossRef](#)] [[PubMed](#)]
3. Radhakrishnan, D.M.; Goyal, V. Parkinson's disease: A review. *Neurol. India* **2018**, *66*, S26–S35. [[CrossRef](#)] [[PubMed](#)]
4. Barbosa, E.R.; Limongi, J.C.; Cummings, J.L. Parkinson's disease. *Psychiatr. Clin. N. Am.* **1997**, *20*, 769–790. [[CrossRef](#)] [[PubMed](#)]
5. Sabat, R.; Dayton, O.L.; Agarwal, A.; Vedam-Mai, V. Analyzing the effect of the COVID-19 vaccine on Parkinson's disease symptoms. *Front. Immunol.* **2023**, *14*, 1158364. [[CrossRef](#)] [[PubMed](#)]
6. Khodakarami, H.; Farzanehfar, P.; Horne, M. The Use of Data from the Parkinson's KinetiGraph to Identify Potential Candidates for Device Assisted Therapies. *Sensors* **2019**, *19*, 2241. [[CrossRef](#)] [[PubMed](#)]

7. Del Rey, N.L.; Quiroga-Varela, A.; Garbayo, E.; Carballo-Carbajal, I.; Fernández-Santiago, R.; Monje, M.H.G.; Trigo-Damas, I.; Blanco-Prieto, M.J.; Blesa, J. Advances in Parkinson's Disease: 200 Years Later. *Front. Neuroanat.* **2018**, *12*, 113. [[CrossRef](#)] [[PubMed](#)]
8. Gumber, A.; Ramaswamy, B.; Ibbotson, R.; Ismail, M.; Thongchundee, O.; Harrop, D.; Allmark, P.; Rauf, A. *Economic, Social and Financial Cost of Parkinson's on Individuals, Carers and Their Families in the UK*; Centre for Health and Social Care Research, Sheffield Hallam University: Sheffield, UK; p. 2017.
9. Piromalis, D.; Papoutsidakis, M.; Tsaramirsis, G. A study of keeping low cost in sensors and μ controller implementations for daily activities. In Proceedings of the 2016 3rd International Conference on Computing for Sustainable Global Development (INDIACom), New Delhi, India, 16–18 March 2016; pp. 1403–1407.
10. Tsaramirsis, G.; Buhari, S.M.; Basher, M.; Stojmenovic, M. Navigating Virtual Environments Using Leg Poses and Smartphone Sensors. *Sensors* **2019**, *19*, 299. [[CrossRef](#)] [[PubMed](#)]
11. Guk, K.; Han, G.; Lim, J.; Jeong, K.; Kang, T.; Lim, E.K.; Jung, J. Evolution of Wearable Devices with Real-Time Disease Monitoring for Personalized Healthcare. *Nanomaterials* **2019**, *9*, 813. [[CrossRef](#)] [[PubMed](#)]
12. Silva de Lima, A.L.; Hahn, T.; Evers, L.J.W.; de Vries, N.M.; Cohen, E.; Afek, M.; Bataille, L.; Daeschler, M.; Claes, K.; Boroojerdi, B.; et al. Feasibility of large-scale deployment of multiple wearable sensors in Parkinson's disease. *PLoS ONE* **2017**, *12*, e0189161. [[CrossRef](#)] [[PubMed](#)]
13. Rovini, E.; Maremmani, C.; Cavallo, F. Automated Systems Based on Wearable Sensors for the Management of Parkinson's Disease at Home: A Systematic Review. *Telemed. e-Health* **2019**, *25*, 167–183. [[CrossRef](#)] [[PubMed](#)]
14. Ancona, S.; Faraci, F.D.; Khatab, E.; Fiorillo, L.; Gnarra, O.; Nef, T.; Bassetti, C.L.A.; Bargiotas, P. Wearables in the home-based assessment of abnormal movements in Parkinson's disease: A systematic review of the literature. *J. Neurol.* **2022**, *269*, 100–110. [[CrossRef](#)] [[PubMed](#)]
15. Banou, E. Kinesia paradoxa: A challenging Parkinson's phenomenon for simulation. *Adv. Exp. Med. Biol.* **2015**, *822*, 165–177. [[CrossRef](#)] [[PubMed](#)]
16. BioSensics. BioSensics. Available online: <https://biosensics.com/> (accessed on 20 March 2024).
17. Kim, T.K. T test as a parametric statistic. *Korean J. Anesthesiol.* **2015**, *68*, 540–546. [[CrossRef](#)] [[PubMed](#)]
18. Kaufmann, J.; Schering, A. Analysis of Variance ANOVA. In *Wiley StatsRef: Statistics Reference Online*; John and Wiley and Sons: Hoboken, NJ, USA, 2014.
19. Andy, F. *Discovering Statistics Using IBM SPSS Statistics*; SAGE Publications: Thousand Oaks, CA, USA, 2017.
20. Nagasubramanian, G.; Sankayya, M.; Al-Turjman, F.; Tsaramirsis, G. Parkinson Data Analysis and Prediction System Using Multi-Variant Stacked Auto Encoder. *IEEE Access* **2020**, *8*, 127004–127013. [[CrossRef](#)]

Disclaimer/Publisher's Note: The statements, opinions and data contained in all publications are solely those of the individual author(s) and contributor(s) and not of MDPI and/or the editor(s). MDPI and/or the editor(s) disclaim responsibility for any injury to people or property resulting from any ideas, methods, instructions or products referred to in the content.